Ecosystem Services 56 (2022) 101448

Contents lists available at ScienceDirect

Ecosystem Services

journal homepage: www.elsevier.com/locate/ecoser

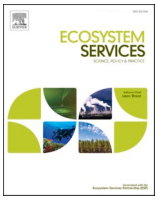

Full Length Article

Mapping ecosystem service supply and demand dynamics under rapid urban expansion: A case study in the Yangtze River Delta of China

Yu Tao [a,b,1], Qin Tao [a,1], Xiao Sun [c], Jiangxiao Qiu [d], Steven G. Pueppke [e,f], Weixin Ou [a,b,*], Jie Guo [a,b], Jiaguo Qi [f]

[a] College of Land Management, Nanjing Agricultural University, Nanjing 210095, China
[b] National & Local Joint Engineering Research Center for Rural Land Resources Use and Consolidation, Nanjing 210095, China
[c] Institute of Agricultural Resources and Regional Planning, Chinese Academy of Agricultural Sciences, Beijing 100081, China
[d] School of Forest, Fisheries, and Geomatics Sciences, Fort Lauderdale Research and Education Center, University of Florida, Davie, FL 33314, USA
[e] Asia Hub for Water-Energy-Food Nexus, Nanjing 210095, China
[f] Center for Global Change and Earth Observations, Michigan State University, East Lansing, MI 48824, USA

ARTICLE INFO

Keywords:
Ecosystem services
Carbon sequestration
Nature-based recreation
Supply and demand
Urban expansion
Land use change

ABSTRACT

Much remains to be learned about the contributions of urban expansion to the supply–demand budgets of ecosystem services (ES), a relationship that is crucial for achieving more sustainable urbanization. To fill this knowledge gap, we mapped supply and demand dynamics of two important ES (i.e., carbon sequestration and nature-based recreation) at 1-km resolution in the rapidly urbanizing Yangtze River Delta (YRD) of China. Carbon sequestration supply (CS_S) and demand (CS_D) were estimated under alternative carbon reduction policies, and supply (NR_S) of and demand (NR_D) for nature-based recreation were estimated by considering multiple levels of spatial accessibility. A moderate increase in CS_S between 2000 and 2015 was contrasted with a sharp increase in CS_D, indicating the existence of a widening gap between demand and supply in the YRD. Urban expansion was responsible for nine-tenths of the total increase in CS_D and two-thirds of the growth in deficit area. As of 2015, CS_S offset less than 5% of CS_D in the eight core cities of the YRD. The areas of deficient CS_S in these eight cities expanded by 8% under the long-term carbon neutrality goal, but they shrank by 34% due to significant decreases in carbon emissions per unit of GDP under the mid-term carbon reduction goal. NR_S in the YRD decreased slightly coincident with moderate increases in NR_D during the same period as a result of urban expansion and population growth. More than half of the increased deficit area was attributable to urban expansion across the region. NR_D in the eight core cities equaled four-fifths of NR_S in 2000, but it surpassed NR_S by one-fifth in 2015. The disparities between NR_S and NR_D in these eight cities were reduced with increasing levels of accessibility to ecological land. Bridging the gaps between supply of and demand for these two ES will require control of unsustainable urban expansion, construction of urban-to-rural greenways, and improved economic efficiency of industrial carbon emissions in the YRD. The analytical framework and methods for mapping ES used here are applicable to other rapidly urbanizing regions of the world.

1. Introduction

The supply of ecosystem services (ES) refers to the capacity of nature to generate and deliver products and benefits to humans (Daily et al., 2000). ES supply has become one of the core concepts and critical indicators for measuring ecosystem quality and health since the Millennium Ecosystem Assessment (2005), and research on ES supply has grown rapidly over the past two decades (Costanza et al., 2017). Recently, increasing attention has been given to the integration between ES supply and demand owing to intensified human-nature interactions around the world (Wei et al., 2017). The demand for provisioning ES is commonly defined and estimated as the sum of ecosystem goods and commodities (e.g., freshwater, food, and raw materials) consumed per unit of space and time (Burkhard et al., 2012). In comparison, the

* Corresponding author at: College of Land Management, Nanjing Agricultural University, Nanjing 210095, China.
E-mail address: owx@njau.edu.cn (W. Ou).

[1] These authors contributed equally to this work. Author contributions: Y. Tao and Q. Tao designed and performed research; Q. Tao and Y. Tao analyzed data; and Y. Tao and Q. Tao wrote the paper.

https://doi.org/10.1016/j.ecoser.2022.101448
Received 3 December 2021; Received in revised form 21 May 2022; Accepted 30 May 2022
Available online 4 June 2022

demand for regulating and cultural ES is often understood as the amount of regulation needed to meet predetermined conditions, or human preferences for desirable environmental conditions, such as clear water and a mild climate, or accessibility and enjoyment of cultural benefits provided by ecosystems (Villamagna et al., 2013). Although it remains challenging to quantify the supply–demand budgets (i.e., differences between the supply and demand sides) of these latter two non-commodity services (Burkhard et al., 2012; Wolff et al., 2015), several studies have attempted to address this issue by focusing on carbon sequestration and nature-based recreation, i.e., the two important ES in human-dominated landscapes (Liu et al., 2020; Yu et al., 2021).

Carbon sequestration has supply (CS_S) and demand (CS_D) components. CS_S is defined as the amount of CO_2 captured and stored by ecosystems over a defined period of time. This can be estimated with a number of biophysical models. For example, the InVEST (Integrated Valuation of Ecosystem Services and Tradeoffs) model estimates carbon storage by using the look-up table method, and CS_S is calculated as changes in carbon storage from vegetation and soil carbon pools when there are changes in land use (Lorilla et al., 2019). CASA is a process-based model which uses solar radiation, soil property, and remote sensing data (e.g., vegetation index) to model ecosystem processes such as carbon uptake and net primary productivity to represent CS_S (Cui et al., 2019). I-tree is an empirical model that estimates CS_S based on tree canopy cover and length of growing season in urban areas (Baró et al., 2015). CS_D is in most cases measured as the sum of CO_2 emissions from consumption of fossil fuels in different socio-economic sectors (Lin et al., 2021). This often leads to an overestimation, because carbon reduction policies allow a proportion of CO_2 emissions, and these should be excluded in estimating CS_D (Chen et al., 2019). In addition, many studies quantify CS_D only at the city-level, because CO_2 emissions data are collected and computed at such scales based on reports from governmental agencies (Sun et al., 2019; Yu et al., 2021). It is much more complicated to allocate citywide estimations of CS_D to spatial grid cells based on the distribution of population (González-García et al., 2020), land use (Chen et al., 2019), and gross domestic product (GDP) (Shi et al., 2020).

The supply of nature-based recreation (NR_S) can be quantified by measuring a number of potential and recreational opportunity factors, including the naturalness of land cover, landscape diversity, the presence of water bodies and protected areas, and proximity to roads and residential areas (Vallecillo et al., 2019; Bing et al., 2021). The demand for nature-based recreation (NR_D) can be measured based on the frequency of use by people, such as the number of visitors or the number of geo-tagged social media photos in each region (Cui et al., 2019; Meng et al., 2020). However, the results of these approaches are not directly comparable owing to inconsistent units of measurement. Better integration of NR_S and NR_D under the same framework can be achieved by simply estimating NR_S as the total area of green spaces within a given district, and estimating NR_D as total population multiplied by the area of green spaces needed per capita (Baró et al., 2016; Liu et al., 2020). This method assumes that all green spaces are equally available to every resident within the district, and that the residents do not have access to green spaces beyond the district. But in fact, local green spaces can be readily shared by residents in neighboring districts, and vice versa. Therefore, such cross-boundary interactions and the levels of accessibility should be considered in order to accurately estimate NR_S in a given district.

Beyond just estimating ES supply and demand, it can be even more challenging to map their budgets at a suitable spatial resolution or scale. This inevitably requires a clear understanding of the spatial relations between service providing and benefiting areas (Herreros-Cantis and McPhearson, 2021). Here, the service providing areas include the spatial units from which ES are sourced, whereas the service benefiting areas are where ES are needed or readily used or consumed (Serna-Chavez et al., 2014). Various ES can show distinctly different relations between providing and benefiting areas, which has strong implications for developing ES-specific approaches to map their supply–demand budgets (Fisher et al., 2009). For example, the provision of hydrologic ES (e.g., flood regulation, water purification) in the upstream areas normally benefits downstream areas along water flow directions within a basin, and it would be suitable to integrate and map the supply of and demand for these hydrologic ES at the sub-basin or basin scale (Stürck et al., 2014). Similarly, the provision of nature-based recreation service from green spaces benefits people in local or adjacent regions through the connection of road networks. Accordingly, the supply–demand budgets of this service are usually mapped for each community or grid cell (Liu et al., 2020). In comparison, the carbon sequestration service is provided omni-directionally and benefits the whole globe, which implies that the demand for carbon sequestration (i.e., carbon emissions) can be offset anywhere on the globe (Bagstad et al., 2014). It is therefore policy-relevant to gain an overview of carbon budget at global to regional scales, and at the same time map carbon budget across local areas (e.g., grid cells) to identify spatially explicit locations with supply–demand mismatches and inform place-based carbon reduction policies for ultimately achieving carbon neutrality on the macro-scale.

There is growing interest in the comprehensive evaluation of supply and demand dynamics of ES in response to rapid urbanization, especially for developing countries like China, where ES supply and demand have been quantified using numerous indicators and methods. For example, Pan and Wang (2021) adopted the indicators of ecological carrying capacity and ecological footprint to represent ES supply and demand, respectively. Tao et al. (2018) developed land cover-based matrices to measure the intensity of ES supply and demand from 0 to 5 for different land covers. Xin et al. (2021) quantified ES supply based on ES values per unit area for each land use, and they quantified ES demand by integrating population, land use, and GDP intensity. Regardless of how ES were quantified, most case studies confirm intensified supply scarcity of ES under rapid urbanization (Bryan et al., 2018), as well as intensified mismatches (i.e., spatially explicit oversupply and undersupply of ES) between ES supply and demand along the urban–rural gradient (Vigl et al., 2017; Deng et al., 2021; Zhang et al., 2021). In spite of these general findings, the dynamic relationships between urbanization and the budgets between supply and demand of ES remain poorly understood. This is due to the lack of spatially explicit approaches to quantify the budgets between ES supply and demand, as well as poor linkages between ES budgets and urban expansion at a fine level of resolution.

Here we examine the rapidly urbanizing Yangtze River Delta (YRD) of China to quantitatively address two key questions: To what extent does urban expansion contribute to temporal changes in ES supply, demand, and budgets? And where exactly do these changes/impacts take place? Our goals include (i) developing spatially explicit models for mapping the supply, demand, and budgets of carbon sequestration and nature-based recreation at a fine spatial resolution, (ii) quantifying the impacts of urban expansion on matches or mismatches between supply and demand of these two ES over space and time, and (iii) proposing land management strategies for bridging the gaps between ES supply and demand under rapid urban expansion.

2. Materials and methods

2.1. Study area

The YRD is located in the coastal region of eastern China (114°54′-123°10′E, 35°20′-27°02′N) and has a total area of 358,000 km^2. Although the north is characterized by flat terrain suitable for agricultural production and urban development, the southern part is dominated by mountainous areas (Fig. 1). The YRD encompasses the Shanghai municipality as well as Jiangsu, Zhejiang, and Anhui provinces, representing one of the most populous and developed regions in China. As of 2015, this region supported 16% of the nation's population and produced nearly one-quarter of its GDP with less than 4% of the country's land area (Yu et al., 2021). Shanghai, Nanjing, Hangzhou, Hefei,

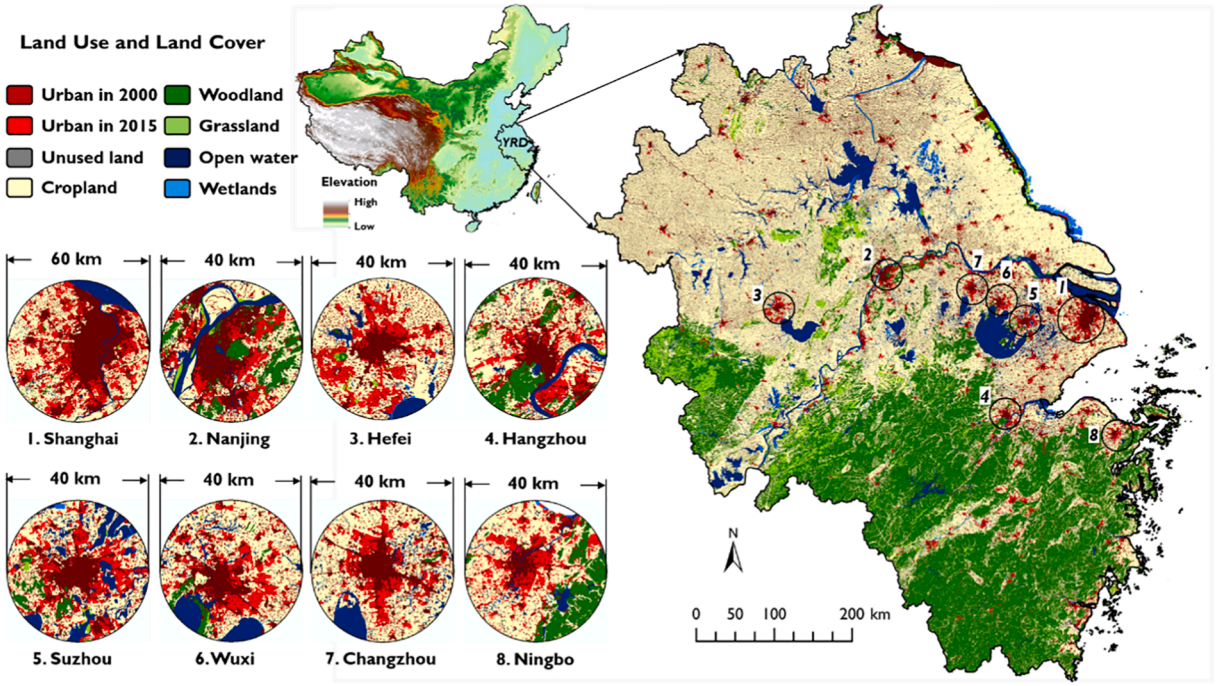

Fig. 1. Land use and land cover of the Yangtze River Delta and urban areas of the eight core cities as of 2015. The urban areas of all cities except Shanghai could be enclosed within circles with diameters of 40 km. A larger diameter, 60 km, was necessary to enclose the urban area of the largest city, Shanghai.

Suzhou, Wuxi, Changzhou, and Ningbo are the eight largest cities of the core YRD in terms of urban land area (Fig. 1 and Table S1). The circular regions surrounding the centroid of these eight cities accounted for 30% of urban land area in the YRD after 15 years of consecutive expansion at an annual rate of 3% between 2000 and 2015 (Tao et al., 2018). Such rapid urbanization has triggered demand for green spaces and generated pressure to reduce CO_2 emissions (Chen et al., 2019), but it has also decreased ecosystem productivity (Xu et al., 2014) and exacerbated supply and demand mismatches of critical ES. For these reasons and as described in detail below, we consequently analyzed these eight cities as a separate cohort.

2.2. Data gathering and pre-processing

Five major YRD datasets were used in this study. (1) Land cover data for the years 2000 and 2015 were produced by the Institute of Remote Sensing and Digital Earth, Chinese Academy of Sciences through interpretation of Landsat TM or ETM images at 30-m resolution (Fig. 1). Urban land, unused land, cropland, grassland, woodland, wetlands, and open water were classified with an overall accuracy of 85% relative to that from ground-based survey data (Liu et al., 2014). (2) Net Primary Productivity (NPP) products were downloaded from the MODIS Website (https://modis.gsfc.nasa.gov) at 1-km resolution for estimation of carbon sequestration between 2000 and 2015. (3) The CO_2 emissions from the industrial, service, transport, household, and agricultural sectors of each city (i.e., an administrative unit) in the YRD in the years 2005 and 2015 were obtained from Cai et al. (2019a, 2019b) based on the China High-Resolution Emission Database (CHRED), statistical data and onsite surveys. By assuming constant CO_2 emissions per unit of GDP between 2000 and 2005, this study further estimated city-level CO_2 emissions in 2000 (E_{2000}) by correcting CO_2 emissions data in 2005 (E_{2005}) with the GDP_{2000}-to-GDP_{2005} ratio of each city as follows:

$$E_{2000} = E_{2005} \bullet \frac{GDP_{2000}}{GDP_{2005}}$$

(4) Nighttime lights time series datasets during 2000–2015 were provided by NOAA's National Centers for Environmental Information (https://www.ngdc.noaa.gov) at 1-km resolution for allocating city-level CO_2 emissions to every urban pixel. (5) Gridded GDP and population products in the years 2000 and 2015 of the YRD were obtained from the Data Center for Resources and Environmental Sciences, Chinese Academy of Sciences (http://www.resdc.cn). These datasets were produced in two major steps. First, the GDP and population data of each city were obtained from the statistical yearbooks in the years 2000 and 2015. Second, the city-level statistical data on GDP and population were spatially distributed to every 1-km grid cell of each city based on land cover and nighttime lights intensity maps. These gridded GDP and population datasets were employed in this study to estimate ES demand at 1-km resolution. All of the 1-km gridded datasets described above, including nighttime lights, NPP, GDP, and population were aligned and resampled using the nearest neighbor algorithm for further manipulation (Fig. S1).

2.3. Mapping carbon sequestration supply and demand

The supply of carbon sequestration refers to the annual capacity of vegetation to absorb and remove CO_2 from the atmosphere. It was quantified using the NPP products obtained in the years 2000 and 2015 (Fig. 2). The amount of sequestered CO_2 in each 1-km grid cell (CS_S) was calculated by multiplying NPP by 1.63, the commonly accepted conversion factor to estimate CO_2 sequestration from NPP (Chen et al., 2019).

$$CS_s = 1.63 \times NPP$$

The demand for carbon sequestration (CS_D) refers to the annual amount of anthropogenic CO_2 emissions that must be reduced to meet relevant carbon reduction goals. Using city-level CO_2 emissions data in the years 2000 and 2015, the amount of CO_2 emissions in each 1-km grid cell was calculated in two steps.

First, CO_2 emissions were only attributed to urban and cropland pixels as classified in Fig. 1. Because urban energy use and the consequent CO_2 emissions were closely related to the nighttime lights intensity of urban pixels (Han et al., 2018), we estimated CO_2 emissions in each 30-m urban pixel (E_{urban_pixel}) of a specific city as the sum of CO_2

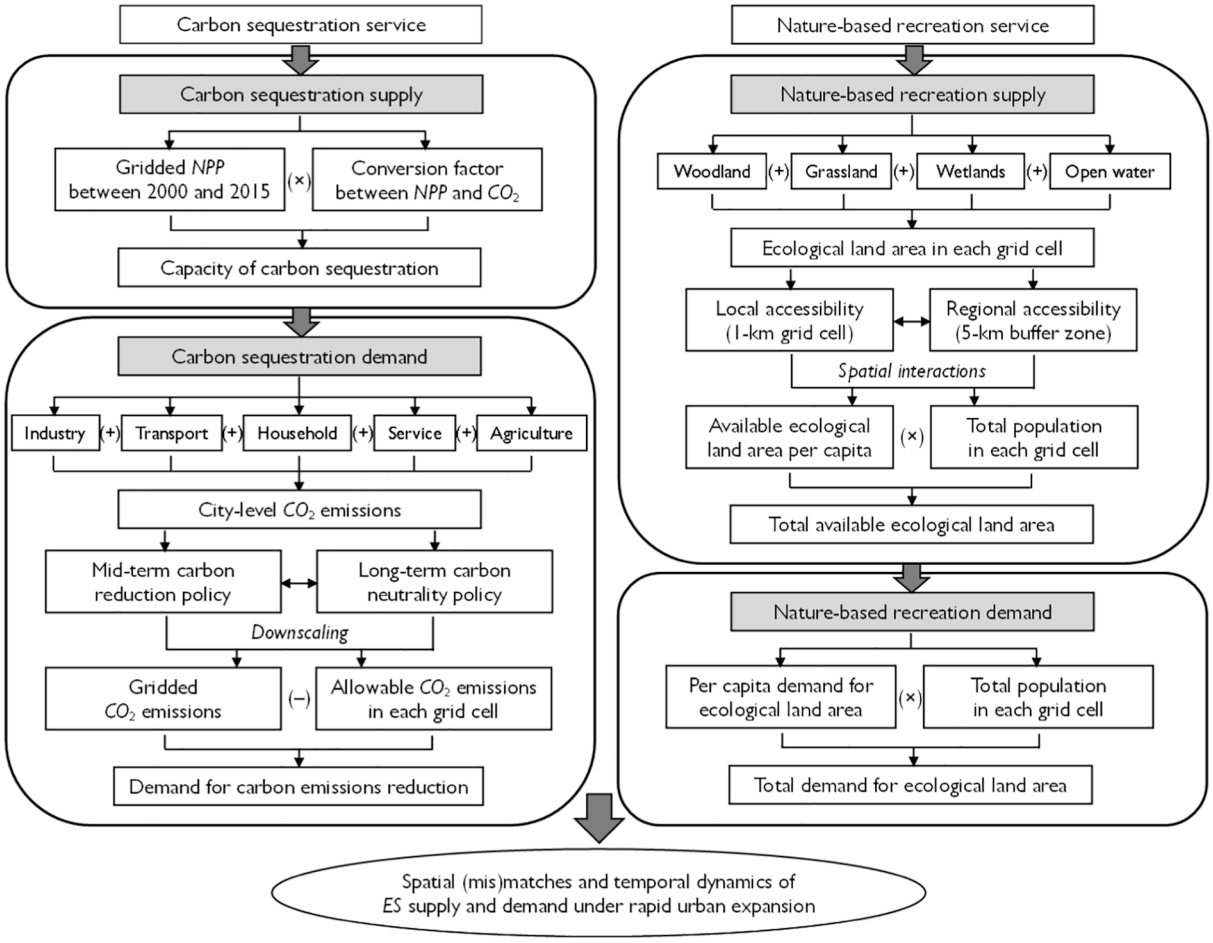

Fig. 2. Assessment framework to integrate supply of and demand for carbon sequestration and nature-based recreation services in the YRD.

emissions from the industrial, service, transport, and household sectors weighted by nighttime lights intensity. Meanwhile, agricultural CO_2 emissions of a specific city were equally distributed to every 30-m cropland pixel (E_{crop_pixel}) in this city using the following equations:

$$E_{urban\_pixel} = (E_{industry} + E_{service} + E_{transport} + E_{household}) \frac{L_{urban\_pixel}}{\sum L_{urban\_pixel}}$$

$$E_{crop\_pixel} = \frac{E_{agriculture}}{N_{crop\_pixel}}$$

where $E_{industry}$, $E_{service}$, $E_{transport}$, $E_{household}$, and $E_{agriculture}$ are CO_2 emissions from industrial, service, transport, household, and agricultural sectors in the city, respectively; N_{crop_pixel} is the number of cropland pixels in the city; L_{urban_pixel} represents the dimensionless nighttime lights (i.e., brightness value) of an urban pixel; and $\sum L_{urban\_pixel}$ is the sum of nighttime lights of all urban pixels in the city. Here the 1-km nighttime light data were first resampled to the 30-m resolution, and they were then aligned with the 30-m urban land cover map using the nearest neighbor algorithm to calculate the nighttime light intensity of each urban pixel.

Second, CO_2 emissions from all 30-m urban and cropland pixels within each 1-km grid cell (E_{grid}) were aggregated using the following equation:

$$E_{grid} = \sum E_{urban\_pixel} + \sum E_{crop\_pixel}$$

On the basis of CO_2 emissions estimates for each grid cell, two national policies on reduction of CO_2 emissions in the medium- and long-term were considered in estimating CS_D (Fig. 2). The mid-term carbon reduction goal requires China and the YRD to reduce CO_2 emissions per unit of GDP by 60% between 2000 and 2030 (Chen and Chen, 2011). Accordingly, the amount of CO_2 emissions that must be sequestered in each grid cell was estimated using the following equations:

$$CS_D = \begin{cases} E_{grid} - E_{goal}, & if\ E_{grid} > E_{goal} \\ 0, & if\ E_{grid} \le E_{goal} \end{cases}$$

$$E_{goal} = \frac{E_{2000}}{GDP_{2000}} \bullet (1 - 0.6) \bullet GDP_i$$

where E_{grid} and E_{goal} are actual and permitted CO_2 emissions in each grid cell; E_{2000} is CO_2 emissions of each grid cell in 2000; E_{2000}/GDP_{2000} represents CO_2 emissions per unit of GDP of each grid cell in 2000; and GDP_i is GDP of grid cells in the year i (i = 2000 or 2015).

In comparison, the long-term carbon neutrality goal requires that all CO_2 emissions, regardless of the amount of GDP produced in that region, must be offset through carbon sequestration as of 2060 (Cai et al., 2021). To accomplish this goal, CS_D is equal to the total amount of CO_2 emissions in each grid cell.

$$CS_D = E_{grid}$$

2.4. Mapping nature-based recreation supply and demand

The supply of nature-based recreation (NR_S) refers to the capacity of natural areas to provide recreational benefits to people. It was measured as the total area of ecological land, defined as woodland, grassland, wetlands, and open water, that was accessible to the residents in each 1-km grid cell. Estimation of NR_S was made at two levels of spatial

accessibility — local and regional (Fig. 2). From a local perspective, ecological land is only accessible to residents within each grid cell. Thus NR_S is equal to the ecological land area of each grid cell (A_{grid}).

$$NR_S = A_{grid} = A_{wood} + A_{grass} + A_{wet} + A_{water}$$

where A_{wood}, A_{grass}, A_{wet}, and A_{water} are the area of woodland, grassland, wetlands, and open water calculated based on land cover data at 30-m resolution in each grid cell.

From a regional perspective, people can travel to access ecological land in adjacent regions. We selected 5 km as the maximum walkable distance to adjacent ecological land and assumed that the ecological land of any grid cell is equally accessible for all residents within the 5-km buffer zone (Liu et al., 2020). Under this assumption, NR_S was estimated using land cover and gridded population data in three steps.

First, the ecological land area of any grid cell shared by every resident within the 5-km buffer zone of that grid cell (A_{per_capita}) was calculated from:

$$A_{per\_capita} = \frac{A_{grid}}{P_{buffer}}$$

where A_{grid} is as defined above and P_{buffer} represents total population within the 5-km buffer zone.

Second, because every resident of a given grid cell can have access to the ecological land from all of the grid cells within its 5-km buffer zone, the ecological land area available for every resident in each given grid cell (S_{per_capita}) was totaled as follows:

$$S_{per\_capita} = \sum_{i=1}^{n} A_{per\_capita\_i}$$

where $A_{per\_capita\_i}$ is the ecological land area of grid cell i shared by every resident; and n is the number of grid cells within the 5-km buffer zone of the given grid cell.

Third, S_{per_capita} was multiplied by total population in the grid cell (P_{grid}) to represent NR_S as the sum of ecological land area available for all the residents in each grid cell:

$$NR_S = S_{per\_capita} \times P_{grid}$$

The demand for nature-based recreation (NR_D) refers to the desire of residents to experience nature for recreational and mental benefits. It is measured at the local scale as the total area of ecological land desired by all of the residents in each grid cell (Fig. 2):

$$NR_D = B_{per\_capita} \times P_{grid}$$

where P_{grid} is as defined above and B_{per_capita} represents the basic ecological land area desired by every resident in a given grid cell. Its value was set at 60 m^2 according to Li and Wang (2004).

2.5. Ecosystem service supply–demand ratio index

As described above, CS_S and CS_D were measured as the amount of sequestered and emitted CO_2, while NR_S and NR_D were measured as the area of accessible and desirable ecological land, respectively. Thus the supply of and demand for either of these two ES were directly comparable with the same unit of measurement. We further quantified ES budgets by developing an ES supply–demand ratio index (ES_R) as follows.

$$ES_R = \begin{cases} \dfrac{ES_S - ES_D}{ES_S}, if\, ES_S \geq ES_D \\ \dfrac{ES_S - ES_D}{ES_D}, if\, ES_S < ES_D \end{cases}$$

where ES_S and ES_D represent supply of and demand for ES in terms of carbon sequestration and nature-based recreation, respectively, and ES_R ranges between −1 and 1. Positive values of ES_R indicate the proportion of ES supply in the grid cell that can be potentially contributed to other regions, while negative values of ES_R indicate the proportion of unmet demand for ES in the grid cell. ES_R values were further subdivided into 20 levels at intervals of 0.1. ES deficient, balanced, and surplus regions were assigned ES_R values ranging between [−1.0, −0.1), [−0.1, 0.1], and (0.1, 1.0], respectively. The calculation and mapping of ES supply, demand, and budgets were conducted using the ArcGIS 10.2 version software.

3. Results

3.1. Spatio-temporal variations in CS_S and CS_D

The calculated amount of sequestered CO_2 in the YRD was 295 Tg in 2000 and 351 Tg in 2015, representing a 19% increase in CS_S (Fig. 3a). This was probably due to proliferation of vegetative growth under the favorable environmental conditions, such as increased annual precipitation and temperature that characterized this period of 2000–2015 (Wu et al., 2014).

Under the mid-term carbon reduction goal, CS_D tripled from 315 Tg in 2000 to 964 Tg in 2015 (Fig. 3b). As a result, the supply–demand ratio decreased from −0.06 in 2000 to −0.64 in 2015 (Fig. 3c), which indicates that CS_S was 94% of CS_D in 2000 but only 36% of CS_D in 2015. The overall gap between CS_S and CS_D in the YRD is consequently widening. In comparison, areas of deficient CS_S accounted for 16% of the total land area in 2000, but this number decreased to 10% in 2015 (Fig. 3d). This tendency was also evident in Fig. 4a and 4b, as the supply–demand ratio changed from negative to positive (i.e., red to green) in many core urban areas, such as Shanghai, Suzhou, and Hangzhou due to rapid economic growth and sharp decreases in CO_2 emissions per unit of GDP by over 60% during 2000–2015.

Under the long-term carbon neutrality goal, CS_D dramatically increased by nearly threefold from 525 Tg in 2000 to 1820 Tg in 2015 (Fig. 3b), while the supply–demand ratio decreased from −0.44 to −0.81 during the same period (Fig. 3c). These results indicate that CS_S met about half of the CS_D in 2000, but only about one-fifth of it in 2015. This was likely due to an explosive increase of CO_2 emissions in the YRD. Areas of deficient CS_S accounted for about 20% of the total land area and remained relatively stable between 2000 and 2015 (Fig. 3d), but the level of deficiency increased from low (light green) to high (bright red) in these deficit areas (Fig. 4c and 4d). In general, urban areas were hotspots of CO_2 emissions where CS_D far exceeded CS_S. Vegetated areas, including woodland, grassland, and cropland were the primary contributors to CS_S in areas with low CS_D, and water areas exhibited a balance between low levels of CS_S and CS_D (Fig. 4).

For the eight core cities, CS_S amounted to 5 Tg in 2000 and 2015, which accounted for less than 2% of the total CS_S in the YRD (Fig. 3e). Under the mid-term carbon reduction goal, CS_D from these cities more than doubled from 98 Tg in 2000 to 206 Tg in 2015 (Fig. 3f). Consequently, the supply–demand ratio decreased slightly from −0.95 in 2000 to −0.98 in 2015 (Fig. 3g), implying that CS_S offset less than 5% of CS_D in these eight core cities. In comparison, areas of these cities with deficient CS_S shrank from 73% to 48% of the total land area between 2000 and 2015 (Fig. 3h). This is attributable to sharply reduced CO_2 emissions per unit of GDP and thus decreased CS_D in the eight core urban areas (Fig. 4a and 4b). Under the long-term carbon neutrality goal, CS_D more than tripled from 164 Tg in 2000 to 507 Tg in 2015 (Fig. 3f). The supply–demand ratio was lower than −0.99 as of 2015 (Fig. 3g), and the areas of deficient CS_S (e.g., mostly urban areas) expanded from 79% to 85% of the total land area during 2000–2015 (Fig. 3h, 4c, and 4d). There was consequently a huge gap between CS_S and CS_D in these eight cities.

3.2. Contributions of urban expansion to CS_S and CS_D budgets

We examined urban areas that expanded between 2000 and 2015 to

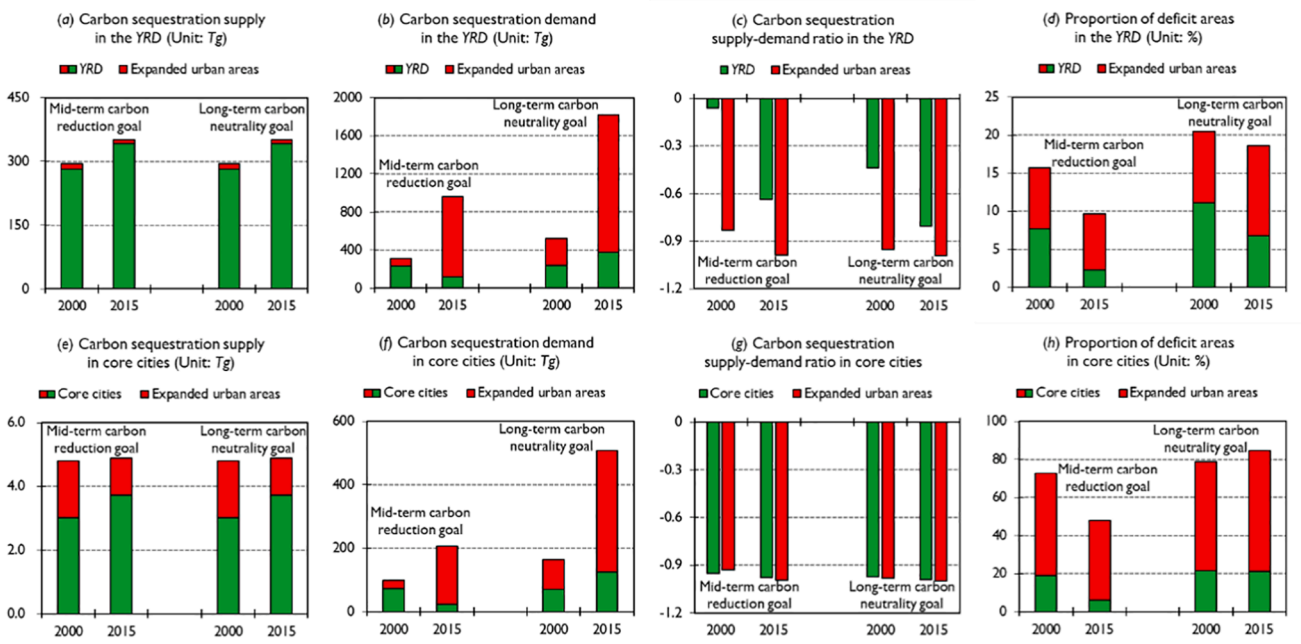

Fig. 3. Carbon sequestration supply, demand, and budgets (i.e., supply–demand ratio) in the YRD and the eight core cities under alternative carbon reduction policies. Expanded urban areas refer to the areas that underwent urban expansion between 2000 and 2015.

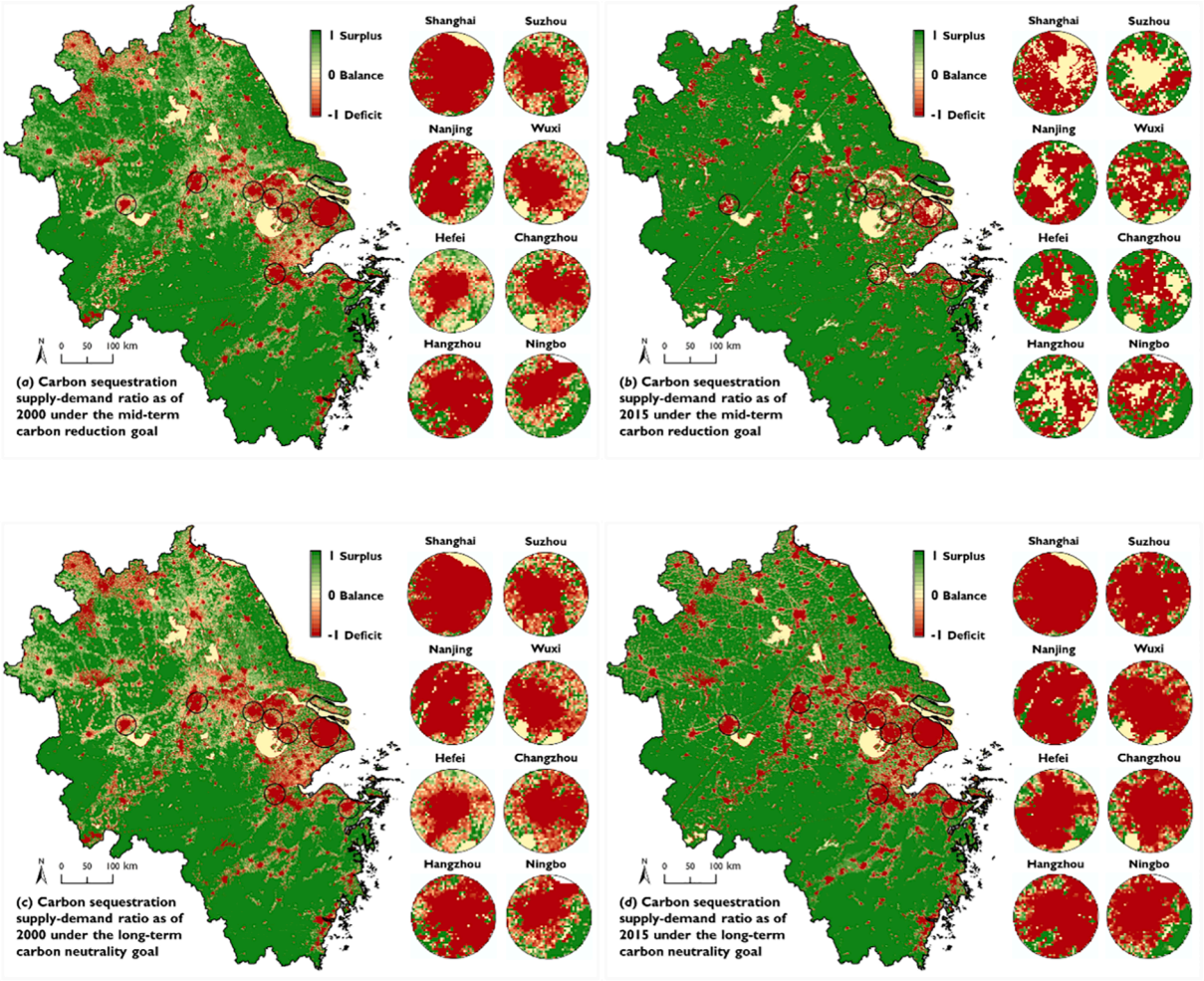

Fig. 4. Spatial (mis)matches between supply of and demand for carbon sequestration in the YRD and the eight core cities under alternative carbon reduction policies. The diameters of the enlarged circles equal 60 km for Shanghai and 40 km for the other seven cities.

explicitly quantify the contributions of such expansion to CS_S and CS_D budgets. Spatial overlaps between these expanded urban areas and expanded deficit areas were also extracted to track the contributions of urban expansion to the growth of deficit areas.

About 3% of the total land area in the YRD was subject to urban expansion between 2000 and 2015. CS_S within these expanded urban areas decreased by 4 Tg, which accounted for 7% of the net increase in CS_S over the entire YRD (Fig. 3a). Under the mid-term carbon reduction goal, CS_D within the expanded urban areas increased by 760 Tg between 2000 and 2015. In comparison, CS_D of the entire YRD grew by only 649 Tg during the same period (Fig. 3b), and thus CS_D in the non-urbanizing regions must have simultaneously decreased by 111 Tg (or 48%). Under the long-term carbon neutrality goal, CS_D within the expanded urban areas increased by 1161 Tg between 2000 and 2015, which accounted for 90% of the net increase in the entire YRD (Fig. 3b). About nine-tenths of the increase in CS_D under the long-term goal is consequently attributable to intensified CO_2 emissions associated with urban expansion, which also contributed two-thirds of the total increase in the deficit area (Fig. 3d).

We also examined the expanded urban areas within the eight core cities of the YRD. Urban expansion consumed 18% of the land area in the eight core cities between 2000 and 2015. CS_S within these expanded urban areas decreased by 0.6 Tg, which was six times larger than the net increase of CS_S in the entire areas of these eight cities (Fig. 3e). Under the mid-term carbon reduction goal, CS_D within the expanded urban areas increased by 157 Tg between 2000 and 2015, which surpassed the net increase of CS_D by 45% in all areas of these eight cities (Fig. 3f). Under the long-term carbon neutrality goal, urban expansion contributed 85% of the total increase in CS_D and 79% of the growth in deficit area in these eight cities (Fig. 3f and 3h).

3.3. Spatio-temporal variations in NR_S and NR_D

The ecological land area of the YRD totaled 137,551 km^2 in 2000 and 136,649 km^2 in 2015, representing a 902 km^2 decrease of NR_S due to urban expansion (Fig. 5a). During the same interval, population growth increased demand for ecological land area (NR_D) by 13%, from 11,708 km^2 to 13,288 km^2 (Fig. 5b). Although NR_D was only about one-tenth of NR_S between 2000 and 2015 (Fig. 5c), areas of deficient NR_S accounted for 26~43% of the total land area in the YRD (Fig. 5d). These deficit areas were dominated by urban and cropland areas in the northern plains (Fig. 6).The situation was much different for the eight core cities, where NR_D dramatically increased by 48% from 1,753 km^2 to 2,595 km^2 over the same period of study (Fig. 5f). As of 2015, these eight cities occupied only 3% of the total land area, but they were responsible for a disproportionate 20% of the NR_D in the entire region owing to their very high and increasing population density.

When defined in terms of local accessibility within each 1-km grid cell, NR_S in these eight cities totaled 2,000 km^2 with a slight decrease between 2000 and 2015 (Fig. 5e). Simultaneously, the supply–demand ratio decreased from +0.13 in 2000 to −0.23 in 2015 (Fig. 5g). This indicates that demand for local access to ecological land, which exhausted only 87% of supply in 2000, surged such that it exceeded supply by 23% just 15 years later. As a consequence, more than 70% of the total land area was classified as deficient as of 2015 (Fig. 5h). If, on the other hand, supply of ecological land is based on the criterion of nearby accessibility, i.e. its location within a walking distance of 5 km, then NR_S in the eight cities was 7% greater as compared to that with local accessibility (Fig. 5e). The supply–demand ratio decreased during this same interval from +0.19 to −0.17 as an overabundant supply of nearby ecological land became exhausted (Fig. 5g). Coincidentally, areas of deficient supply expanded from 48% to 57% of the total land area in these eight cities (Fig. 5h).

3.4. Contributions of urban expansion to NR_S and NR_D budgets

The influence of urban expansion on NR_S and NR_D were quantified following the approaches presented in the Section 3.2. The expanded urban areas of the YRD experienced a moderate 15~26% decrease in NR_S, but a dramatic 86% increase in NR_D during 2000–2015. As of 2015, these expanded urban areas contributed only 5% of the total NR_S of the YRD, but they represented 27% of the total NR_D in the region (Fig. 5a and 5b). Urban expansion also contributed 50~60% of the increased deficit area in the YRD (Fig. 5d).

For the eight core cities, NR_S of the expanded urban areas decreased by 18~35%, but NR_D more than doubled during 2000–2015. As of 2015, these expanded urban areas contributed about one-fifth of the total NR_S but one-half of the total NR_D (Fig. 5e and 5f). In addition, over 70% of

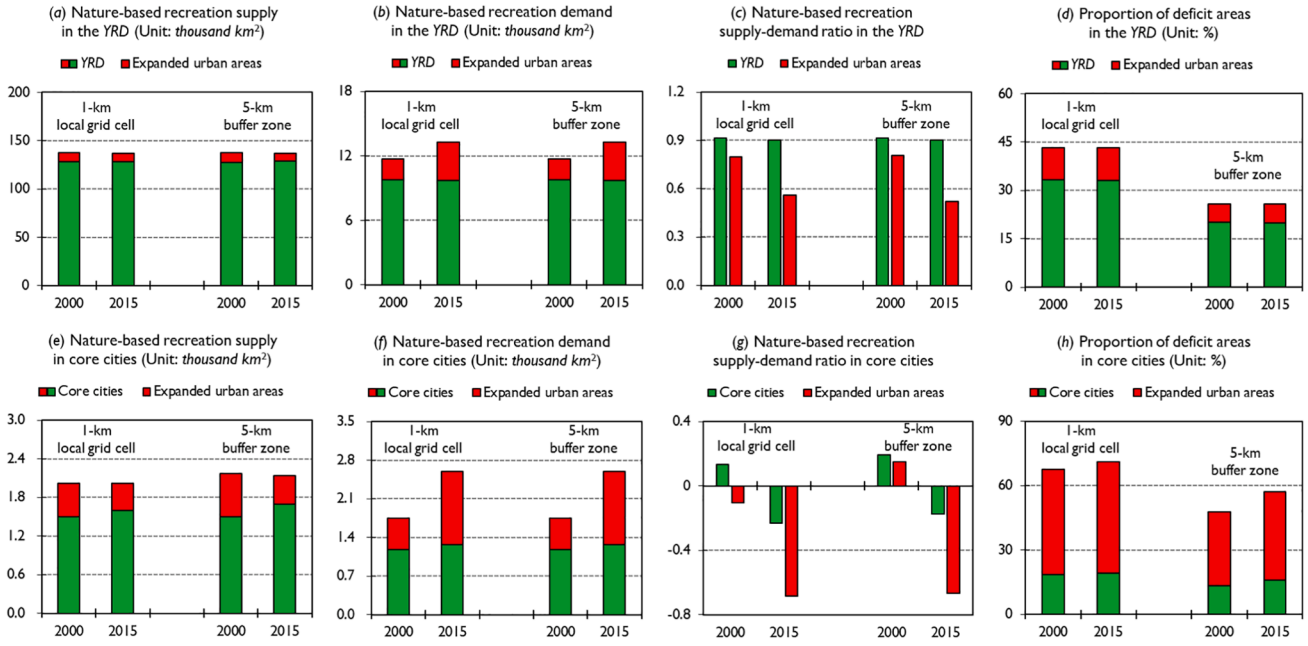

Fig. 5. Nature-based recreation supply, demand, and budgets (i.e., supply–demand ratio) in the YRD and the eight core cities at different levels of accessibility. Expanded urban areas refer to the areas that underwent urban expansion between 2000 and 2015.

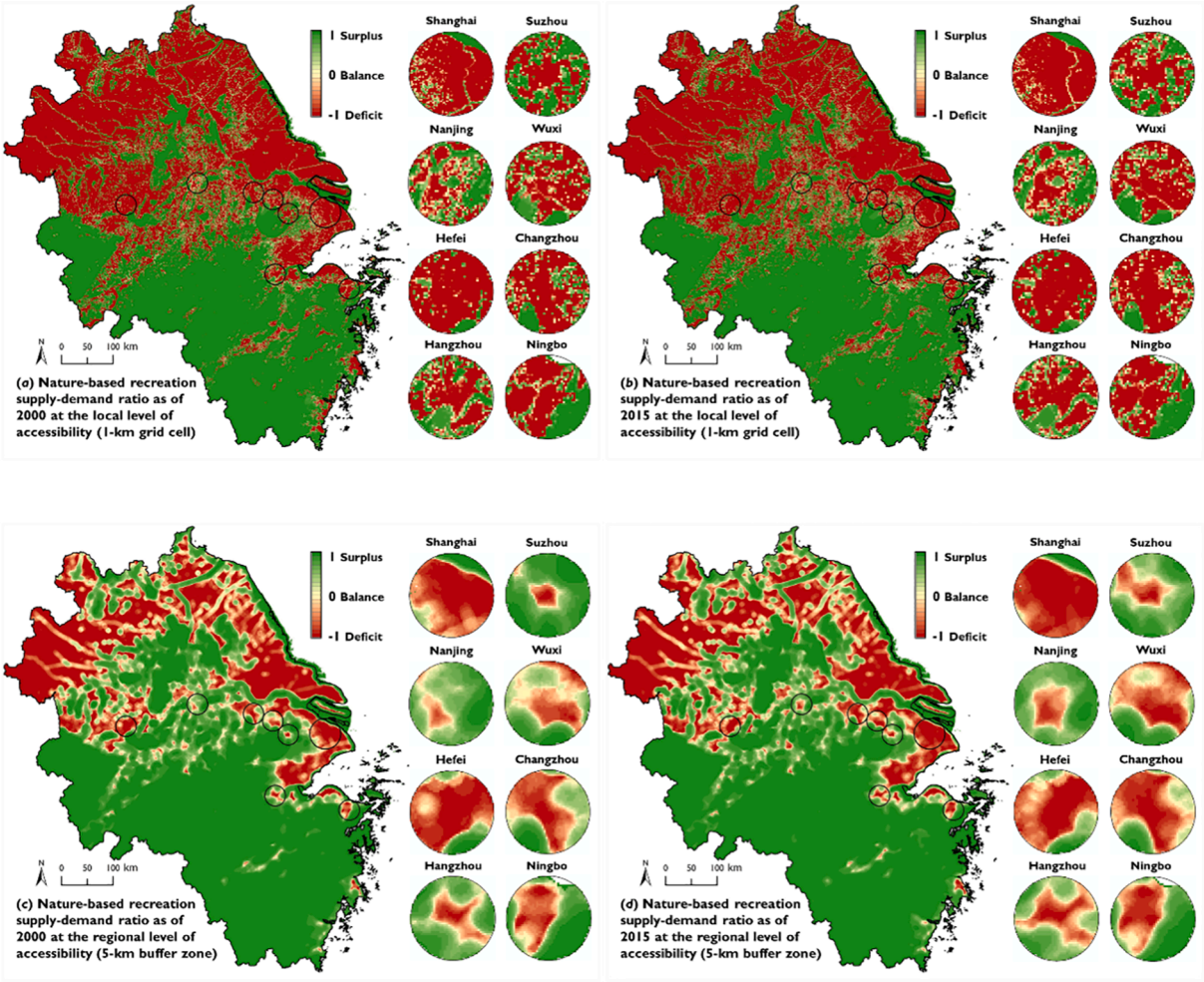

Fig. 6. Spatial (mis)matches between supply of and demand for nature-based recreation in the YRD and the eight core cities at local to regional levels of accessibility. The diameters of the enlarged circles equal 60 km for Shanghai and 40 km for the other seven cities.

the increased deficit area was attributable to urban expansion (Fig. 5h). These findings indicate an even stronger impact of urban expansion on NR_S and NR_D in these eight core cities than over the entire region.

3.5. Key influencing factors of ES supply and demand

As shown in Fig. 7a, on average, cropland, woodland, and urban land contributed 50%, 35%, and 8%, respectively of the CS_S in the YRD during 2000–2015. These three land uses were also the primary sources of CS_S in the eight core cities. Owing to rapid urban expansion and cropland losses, CS_S of urban land increased dramatically from 12% to 25% of the total CS_S in these eight cities between 2000 and 2015, but CS_S of cropland decreased from 69% to 55% of the total CS_S during the same period (Fig. 7f). The CS_S per unit area of woodland, cropland, and urban land in the YRD averaged 9.8, 7.9, and 5.9 tons/ha, respectively (Fig. 7b). In comparison, the CS_S per unit area of these three land uses in the eight core cities averaged only 7.6, 4.9, and 1.9 tons/ha. In each case, the cities significantly underperformed the YRD as a whole, by 22%, 38%, and 68%, respectively (Fig. 7g). This was probably because of development of high density urban areas, cropland fragmentation, and associated cropland abandonment as more rural residents migrate to the urban areas in these rapidly growing cities (Hou et al., 2021).

On the demand side, the quantity of CO_2 emissions is the dominant factor affecting CS_D under the long-term carbon neutrality goal. Based on publicly available datasets (Cai et al., 2019a, 2019b), CO_2 emissions from the industrial and transport sectors accounted for 88% and 8% of the total CO_2 emissions in the YRD, respectively (Fig. 7c). These two sectors also contributed over 95% of the total CO_2 emissions for the eight core cities (Fig. 7h). Between 2000 and 2015, industrial and transport-related CO_2 emissions more than tripled in the YRD, resulting in a parallel increase in total CO_2 emissions. As of 2015, the service sector contributed only 2~3% of the total CO_2 emissions in the YRD and the eight core cities, but these emissions increased exponentially by 8~13 times during 2000–2015 (Fig. 7c and 7h).

Calculation of CO_2 emissions per unit of GDP provides additional information that is directly relevant to the mid-term carbon reduction goal. CO_2 emissions per million yuan of GDP in the YRD decreased from 190 tons in 2000 to 115 tons in 2015, representing a 39% reduction (Fig. 7d). For the eight core cities, this number decreased even faster, by 83% during the same period (Fig. 7i). This means that these cities have already surpassed the national goal of reducing CO_2 emissions per unit of GDP by 60% between 2000 and 2030 (Chen and Chen, 2011). Owing to the rapidly decreased CO_2 emissions per unit of GDP as of 2015, CS_D was lower by 47~59% under the mid-term carbon reduction goal than under the long-term carbon neutrality goal (Fig. 3b and 3f).

The ecological land area per capita is critical in determining NR_S and NR_D, especially for the densely populated urban areas. As shown in Fig. 7e and 7j, the ecological land area per capita in the eight core cities amounted to only one-tenth of that over the entire YRD. Moreover, it decreased by one-third, from 69 m^2 in 2000 to 46 m^2 in 2015, due to urban encroachment and population growth. As a consequence, NR_D increased and surpassed NR_S, and the areas of deficient NR_S expanded

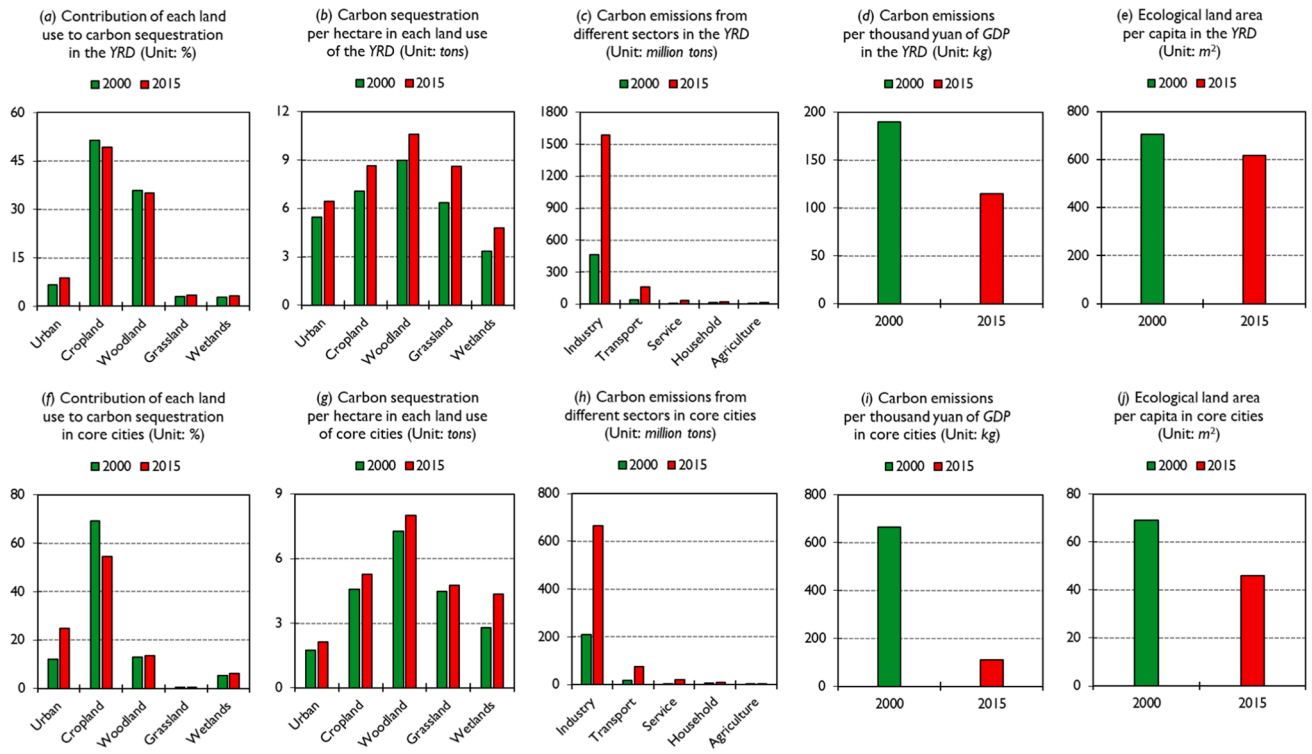

Fig. 7. Key factors that influence the supply of and demand for carbon sequestration and nature-based recreation services in the YRD and the eight core cities.

rapidly in these eight core cities (Fig. 5g and 5h). Our results also highlight the importance of spatial accessibility in estimating NR_S. In general, NR_S of urban areas would increase if ecological land was accessible not only locally but also regionally from a longer distance (Fig. 5e), so that the ecological land resources of adjacent rural areas could be accessed by urban residents.

4. Discussion

4.1. ES supply and demand dynamics are best revealed at high spatial resolution and under multiple scenarios

There has been a growing number of international and Chinese case studies that investigate supply and demand dynamics of ES (e.g., carbon sequestration and nature-based recreation) in hotspots of urbanization. These studies reveal growing disparities over time and intensified mismatches over space between supply of and demand for ES under rapid urbanization of major metropolises, such as New York (Herreros-Cantis and McPhearson, 2021), Barcelona (Baró et al., 2016), Madrid (González-García et al., 2020), Shanghai (Chen et al., 2019), and Guangzhou (Liu et al., 2020).

The results presented here not only confirm that urban expansion is one of the primary contributors to the imbalance between ES supply and demand in the rapidly urbanizing regions of the YRD, but also improve on previous approaches by estimating CS_D with respect to alternative carbon reduction goals. Accordingly, CO_2 emissions per unit of GDP in major urban areas of the YRD were reduced by 83% between 2000 and 2015 (Fig. 7i), which far surpassed the 60% mid-term carbon reduction goal. This in turn led to sharply decreased CS_D between 2000 and 2015 and a reverse in the supply–demand ratio from negative to positive in the core of these urban areas under this mid-term goal (Fig. 4a and 4b). In contrast, every gram of CO_2 emissions should be sequestered regardless of its economic efficiency under the long-term carbon neutrality goal. It is consequently significant that CS_D more than tripled between 2000 and 2015 as supply scarcity intensified from low to high in major urban areas (Fig. 4c and 4d). These policy-relevant estimations of CS_D, in conjunction with CS_S, indicate where and how many of CO_2 emissions should be offset through carbon sequestration under alternative carbon reduction goals, and thus provide a concrete scientific basis to inform adaptive strategies for achieving regional carbon neutrality.

Our study also estimates NR_S for each grid cell at multiple levels of spatial accessibility, so that the influence of neighboring cells is synthesized into the analysis. NR_S increased markedly in major urban areas of the YRD as their access to ecological land extend from local to peripheral grid cells (Fig. 5e). This further influences budgets between NR_S and NR_D, as the areas of deficient NR_S, i.e., those red areas in Fig. 6, decreased from 43% to 26% of the total land area over the YRD, due to increased threshold distance from 1 to 5 km. These accessibility findings consequently highlight the importance of improving connectivity between urban and more peripheral areas in alleviating supply scarcity of NR_S in the urban core.

Whilst most other studies quantify ES supply, demand, and budgets at the city or district level (Sun et al., 2019; Yu et al., 2021), we developed spatially explicit models to map the budgets between ES supply and demand for each 1-km grid cell of the YRD (Figs. 4 and 6). These high resolution maps of ES identify areas of supply scarcity that could be further associated with urban expansion and gridded population and GDP datasets to generate information with strong socio-economic implications. For instance, we estimate that as of 2015, as much as 57% of GDP produced in the YRD negatively affected carbon budgets (Fig. 8a), and up to 65% of the total population was subject to scarce nature-based recreational opportunities (Fig. 8c). There was an even higher proportion of GDP and population located in the ES deficit areas of the eight core cities (Fig. 8b and 8d). These results imply an urgent need to manage ES supply shortfalls and their impact on human well-being in these rapidly urbanizing regions.

4.2. Limitations and prospects for future research

Although our approach has led to new insights about ES supply and demand, it is subject to several limitations. First and foremost, it is

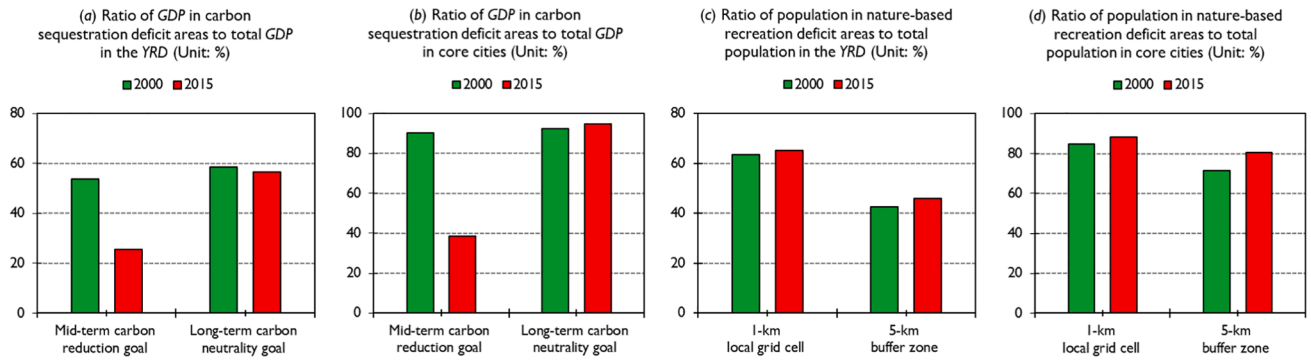

Fig. 8. Distribution of GDP and population in the deficit areas of carbon sequestration and nature-based recreation services.

crucial to acknowledge the spatial relationships between service providing and service benefiting areas (Fisher et al., 2009) that can vary by each service. Such spatial relationships play an essential role in determining the best suitable spatial unit or scale for mapping ES supply–demand budgets. For example, for carbon sequestration service, CS_S is locally provided in each grid cell, but the beneficiaries (e.g., urban and rural residents) are located both within and beyond the scope of each grid cell. Because of this, CS_D does not necessarily need to be offset by CS_S on-site. Here urban grid cells have inherently high CS_D but low CS_S, and it seems infeasible for these urban areas to reach complete carbon neutrality. Therefore, although our 1-km gridded maps present spatially explicit locations of mismatches between CS_S and CS_D, we should be cautious to interpret these results at such a high resolution. In comparison, we might obtain more policy-relevant results simply by focusing on the whole area of study (including both urban and surrounding rural landscapes) to assess budgets between CS_S and CS_D at the regional level. Second, it is challenging to downscale city-level CO_2 emissions data to the pixel level when we attempted to map CS_D at a 1-km resolution. Although urban CO_2 emissions have been positively associated with nighttime lights intensity (Han et al., 2018), use of spatially allocated nighttime lights as a proxy for CO_2 emissions from the industrial, service, transport, and household sectors introduces potential uncertainties. It can be even more complicated to determine agricultural CO_2 emissions from each cropland pixel. We simplified this process by equally allocating CO_2 emissions from the agricultural sector to each cropland pixel, but this, too, introduces uncertainties. It will be important to correct our gridded estimates of CO_2 emissions as more detailed classification of urban land uses and crop types become available in the future. Third, this current study assumed that different grid cells of the YRD share the same carbon reduction goal. But in reality, some grid cells (e.g., those with higher GDP contributions) might need to reduce more CO_2 emissions than the others due to their inherent differences in CO_2 reduction potentials. Thus the accuracy of CS_D estimates could be further improved in follow-up studies that consider any weight indicator (e.g., GDP, population density, nighttime lights intensity) in determining site-specific carbon reduction goals over the YRD.

As to nature-based recreation service, NR_S was measured simply as the total area of available ecological land in this study. This approach neglects ecological land characteristics such as biomass, species richness, size, and shape that are known to influence NR_S (Liu et al., 2021). Moreover, the contiguity among grid cells was assessed using buffer analysis, an approach that can be improved by using road maps to more accurately measure the amount of ecological land available for each grid cell. It would also be much more accurate by applying a decay function (e.g., exponential or logistic based on empirical data) to account for fine-scale service declining pattern in response to distances to ecological land, as the threshold distance applied in this current approach might be equally accessible for all beneficiaries (e.g., 5-km distance might be too long for elderly or physically disabled people) (Miyake et al., 2010). Croplands play a substitutional role in providing nature-based recreational opportunities to urban and rural residents (He et al., 2019), but the contribution of this land cover type to NR_S was not quantified in the present study. This likely contributed to the observed significant shortfalls in NR_S for agricultural areas of the northern YRD (Fig. 6). On the demand side, NR_D was estimated using the ecological land area required per capita for recreation as a proxy. This value was set constant as 60 m^2 per capita (Li and Wang, 2004), but in fact, the individual demand for ecological land area varies from urban to rural regions due to the contrasting levels of income, education, and population density (Zhou et al., 2018). Although challenging, this information could be obtained in future studies by using a participatory approach to assess the perceptions and preferences of local residents.

In addition to mapping ES budgets, analyses of ES dynamics in response to rapid urban expansion were also subject to several limitations. Although we examined the urbanization effects on ES budgets not only for the entire region of study but also for the eight core cities, they were not illustrated separately but rather as one integrative case. Because of this, nuances in urban expansion and consequent changes in ES budgets across these cities were not explicitly revealed. Further efforts would be worthwhile to investigate how urban expansion and its impact on ES budgets differ across a range of cities with varying socio-economic and natural factors, and how these factors contribute to differences in urban expansion effects on ES budgets.

4.3. Policy implications for bridging the gaps between ES supply and demand

Our findings have important implications for the ability of the YRD to meet its overall carbon reduction goals, and it mandates increased attention to rapidly expanding cities that characterize this region. We estimate that the CS_S per unit area of urban land is as much as 75% less than that of woodland and cropland in the eight core cities of the YRD. Although CS_S per unit area of all three land types increased somewhat between 2000 and 2015, this was accompanied by markedly increased emissions from the industrial, transport, and service sectors.

We recommend that steps must be taken to manage the extent and form of urban expansion in these hotspots of urbanization. This should involve concrete measures to limit urban encroachment onto cropland and woodland coupled with policies to promote urban greening. Uncontrolled encroachment that leads to sprawl, which exacerbates transportation needs, must be avoided. There is also considerable room for improvement of economic efficiency, given that as of 2015, 39% of GDP in the eight core cities was produced in areas of carbon sequestration deficiency, i.e., those where CS_D surpassed CS_S (Fig. 8b).

We also recommend that the countermeasures proposed above would enhance the quality of life of urban residents as quantified here in terms of accessibility to nearby and adjacent ecological land. Spatial relationships are critical in this regard. As of 2015, local access, i.e., that within individual 1-km grid cells, met the needs of just 35% of the total population in the YRD, but if adjacency is considered, the needs of 54%

in the total population are met (Fig. 8c). This underscores the importance of urban form and the desirability of connecting densely populated urban areas with peripheral natural areas via greenways.

5. Conclusions

In this study, the supply and demand dynamics of two important ecosystem services (i.e., carbon sequestration and nature-based recreation) were quantified for the rapidly urbanizing YRD of China. Although CS_S is moderately increasing in the YRD, this favorable trend is being more than offset by sharp increases in CS_D. As of 2015, only one-fifth of CS_D in this critical, rapidly developing economic region was offset by CS_S under the long-term carbon neutrality goal. Urban expansion contributed nine-tenths of the total increase in CS_D and two-thirds of the growth in deficit area where CS_D surpassed CS_S. But these deficit areas shrank in major urban areas due to improved economic efficiency of CO_2 emissions per unit of GDP under the mid-term carbon reduction goal. Our results also showed a slight decrease in NR_S but a moderate increase in NR_D over the YRD. Between 2000 and 2015, more than half of the increased deficit area was attributable to urban expansion, these expanded urban areas contributed only 5% of the total NR_S while 27% of the total NR_D in the YRD. As of 2015, NR_D surpassed NR_S by one-fifth in the eight core cities of the YRD. The gaps between NR_S and NR_D in these major urban areas could be reduced by increasing the amount and connectivity of ecological land between urban and its peripheral regions (e.g., 5-km buffer zones).

Declaration of Competing Interest

The authors declare that they have no known competing financial interests or personal relationships that could have appeared to influence the work reported in this paper.

Acknowledgments

The authors are grateful to the anonymous reviewers and editors for their valuable comments and suggestions. This research was supported by the Jiangsu Talent Program for Innovation and Entrepreneurship (JSSCBS20210282); the National Natural Science Foundation of China (41971230); the Strategic Priority Research Program of the Chinese Academy of Sciences (XDA23020201); the Fundamental Research Funds for the Central Universities (KJQN201847); the NAU-MSU Joint Project (2017-AH-10); and the Program of Introducing Talents of Discipline to Universities (B17024).

Appendix A. Supplementary data

Supplementary data to this article can be found online at https://doi.org/10.1016/j.ecoser.2022.101448.

References

Bagstad, K.J., Villa, F., Batker, D., et al., 2014. From theoretical to actual ecosystem services: mapping beneficiaries and spatial flows in ecosystem service assessments. Ecol. Soc. 19 https://doi.org/10.5751/ES-06523-190264.
Baró, F., Haase, D., Gómez-Baggethun, E., et al., 2015. Mismatches between ecosystem services supply and demand in urban areas: a quantitative assessment in five European cities. Ecol. Ind. 55, 146–158.
Baró, F., Palomo, I., Zulian, G., et al., 2016. Mapping ecosystem service capacity, flow and demand for landscape and urban planning: a case study in the Barcelona metropolitan region. Land Use Policy 57, 405–417.
Bing, Z., Qiu, Y., Huang, H., et al., 2021. Spatial distribution of cultural ecosystem services demand and supply in urban and suburban areas: a case study from Shanghai, China. Ecol. Indicators 127, 107720.
Bryan, B.A., Ye, Y., Zhang, J., et al., 2018. Land-use change impacts on ecosystem services value: incorporating the scarcity effects of supply and demand dynamics. Ecosyst. Serv. 32, 144–157.
Burkhard, B., Kroll, F., Nedkov, S., et al., 2012. Mapping ecosystem service supply, demand and budgets. Ecol. Ind. 21, 17–29.
Cai, B., Cao, L., Lei, Y., et al., 2021. China's carbon emission pathway under the carbon neutrality target. China Popul., Resour. Environ. 31, 7–14 in Chinese.
Cai, B., Cui, C., Zhang, D., et al., 2019a. China city-level greenhouse gas emissions inventory in 2015 and uncertainty analysis. Appl. Energy 253, 113579.
Cai, B., Lu, J., Wang, J., et al., 2019b. A benchmark city-level carbon dioxide emission inventory for China in 2005. Appl. Energy 233-234, 659–673.
Chen, J., Chen, X., 2011. A preliminary study on China's long and medium-term strategic goals for reducing carbon emissions. Sino-Global Energy 16, 1–9 in Chinese.
Chen, J., Jiang, B., Bai, Y., et al., 2019. Quantifying ecosystem services supply and demand shortfalls and mismatches for management optimization. Sci. Total Environ. 650, 1426–1439.
Costanza, R., de Groot, R., Braat, L., et al., 2017. Twenty years of ecosystem services: How far have we come and how far do we still need to go? Ecosyst. Serv. 28, 1–16.
Cui, F., Tang, H., Zhang, Q., et al., 2019. Integrating ecosystem services supply and demand into optimized management at different scales: a case study in Hulunbuir, China. Ecosyst. Serv. 39, 100984.
Daily, G.C., Söderqvist, T., Aniyar, S., et al., 2000. The value of nature and the nature of value. Science 289, 395–396.
Deng, C., Liu, J., Liu, Y., et al., 2021. Spatiotemporal dislocation of urbanization and ecological construction increased the ecosystem service supply and demand imbalance. J. Environ. Manage. 288, 112478.
Fisher, B., Turner, R.K., Morling, P., 2009. Defining and classifying ecosystem services for decision making. Ecol. Econ. 68, 643–653.
González-García, A., et al., 2020. Quantifying spatial supply-demand mismatches in ecosystem services provides insights for land-use planning. Land Use Policy 94, 104493.
Han, J.i., Meng, X., Liang, H., et al., 2018. An improved nightlight-based method for modeling urban CO_2 emissions. Environ. Modell. Software 107, 307–320.
He, S., Su, Y., Shahtahmassebi, A.R., et al., 2019. Assessing and mapping cultural ecosystem services supply, demand and flow of farmlands in the Hangzhou metropolitan area, China. Sci. Total Environ. 692, 756–768.
Herreros-Cantis, P., McPhearson, T., 2021. Mapping supply of and demand for ecosystem services to assess environmental justice in New York City. Ecol. Appl. 31, e02390.
Hou, D., Meng, F., Prishchepov, A.V., 2021. How is urbanization shaping agricultural land-use? Unraveling the nexus between farmland abandonment and urbanization in China. Landscape Urban Plann. 214, 104170.
Li, F., Wang, R., 2004. Research advance in ecosystem service of urban green space. Chin. J. Appl. Ecol. 15, 527–531 in Chinese.
Lin, Y., Chen, X., Huang, L., et al., 2021. Fine-scale mapping of urban ecosystem service demand in a metropolitan context: a population-income-environmental perspective. Sci. Total Environ. 781, 146784.
Liu, H., Remme, R.P., Hamel, P., et al., 2020. Supply and demand assessment of urban recreation service and its implication for greenspace planning - A case study on Guangzhou. Landscape Urban Plann. 203, 103898.
Liu, J., Kuang, W., Zhang, Z., et al., 2014. Spatiotemporal characteristics, patterns and causes of land use changes in China since the late 1980s. Acta Geographica Sinica 24 (2), 195–210.
Liu, Z., Huang, Q., Yang, H., 2021. Supply-demand spatial patterns of park cultural services in megalopolis area of Shenzhen, China. Ecol. Indicators 121, 107066.
Lorilla, R.S., Kalogirou, S., Poirazidis, K., et al., 2019. Identifying spatial mismatches between the supply and demand of ecosystem services to achieve a sustainable management regime in the Ionian Islands (Western Greece). Land Use Policy 88, 104171.
Meng, S., Huang, Q., Zhang, L., et al., 2020. Matches and mismatches between the supply of and demand for cultural ecosystem services in rapidly urbanizing watersheds: a case study in the Guanting Reservoir basin, China. Ecosyst. Serv. 45, 101156.
Millennium Ecosystem Assessment, 2005. Ecosystems and Human Well-Being. Island Press, Washington DC.
Miyake, K.K., Maroko, A.R., Grady, K.L., et al., 2010. Not just a walk in the park: methodological improvements for determining environmental justice implications of park access in New York City for the promotion of physical activity. Cities Environ. 3 (1), 1–17.
Pan, Z., Wang, J., 2021. Spatially heterogeneity response of ecosystem services supply and demand to urbanization in China. Ecol. Eng. 169, 106303.
Serna-Chavez, H.M., Schulp, C.J.E., van Bodegom, P.M., et al., 2014. A quantitative framework for assessing spatial flows of ecosystem services. Ecol. Ind. 39, 24–33.
Shi, Y., Shi, D., Zhou, L., et al., 2020. Identification of ecosystem services supply and demand areas and simulation of ecosystem service flows in Shanghai. Ecol. Ind. 115, 106418.
Stürck, J., Poortinga, A., Verburg, P., 2014. Mapping ecosystem services: The supply and demand of flood regulation services in Europe. Ecol. Ind. 38, 198–211.
Sun, W., Li, D., Wang, X., et al., 2019. Exploring the scale effects, trade-offs and driving forces of the mismatch of ecosystem services. Ecol. Ind. 103, 617–629.
Tao, Y., Wang, H., Ou, W., et al., 2018. A land-cover-based approach to assessing ecosystem services supply and demand dynamics in the rapidly urbanizing Yangtze River Delta region. Land Use Policy 72, 250–258.
Vallecillo, S., La Notte, A., Zulian, G., et al., 2019. Ecosystem services accounts: valuing the actual flow of nature-based recreation from ecosystems to people. Ecol. Model. 392, 196–211.
Vigl, L., Depellegrin, D., Pereira, P., et al., 2017. Mapping the ecosystem service delivery chain: capacity, flow, and demand pertaining to aesthetic experiences in mountain landscapes. Sci. Total Environ. 574, 422–436.
Villamagna, A., Angermeier, P., Bennett, E., 2013. Capacity, pressure, demand, and flow: a conceptual framework for analyzing ecosystem service provision and delivery. Ecol. Complexity 15, 114–121.

Wei, H., Fan, W., Wang, X., et al., 2017. Integrating supply and social demand in ecosystem services assessment: a review. Ecosyst. Serv. 25, 15–27.
Wolff, S., Schulp, C., Verburg, P., 2015. Mapping ecosystem services demand: a review of current research and future perspectives. Ecol. Ind. 55, 159–171.
Wu, S., Zhou, S., Chen, D., et al., 2014. Determining the contributions of urbanisation and climate change to NPP variations over the last decade in the Yangtze River Delta, China. Sci. Total Environ. 472, 397–406.
Xin, R., Skov-Petersen, H., Zeng, J., et al., 2021. Identifying key areas of imbalanced supply and demand of ecosystem services at the urban agglomeration scale: a case study of the Fujian Delta in China. Sci. Total Environ. 791, 148173.
Xu, X., Tan, Y., Chen, S., et al., 2014. Changing patterns and determinants of natural capital in the Yangtze River Delta of China 2000–2010. Sci. Total Environ. 466-467, 326–337.
Yu, H., Xie, W., Sun, L., et al., 2021. Identifying the regional disparities of ecosystem services from a supply-demand perspective. Resour. Conserv. Recycl. 169, 105557.
Zhang, Z., Peng, J., Xu, Z., et al., 2021. Ecosystem services supply and demand response to urbanization: a case study of the Pearl River Delta, China. Ecosyst. Serv. 49, 101274.
Zhou, T., Koomen, E., van Leeuwen, E., 2018. Residents' preferences for cultural services of the landscape along the urban-rural gradient. Urban For. Urban Greening 29, 131–141.